

Intra-Layer Nonuniform Quantization of Convolutional Neural Network

Fangxuan Sun, Jun Lin, and Zhongfeng Wang

School of Electronic Science and Engineering, Nanjing University, China

Email: njusunfx@gmail.com, {jlin, zfwang}@nju.edu.cn

Abstract—Deep convolutional neural network (DCNN) has achieved remarkable performance on object detection and speech recognition in recent years. However, the excellent performance of a DCNN incurs high computational complexity and large memory requirement. In this paper, an equal distance nonuniform quantization (ENQ) scheme and a K-means clustering nonuniform quantization (KNQ) scheme are proposed to reduce the required memory storage when low complexity hardware or software implementations are considered. For the VGG-16 and the AlexNet, the proposed nonuniform quantization schemes reduce the number of required memory storage by approximately 50% while achieving almost the same or even better classification accuracy compared to the state-of-the-art quantization method. Compared to the ENQ scheme, the proposed KNQ scheme provides a better tradeoff when higher accuracy is required.

Index Terms—deep learning, convolutional neural network, quantization, k-means clustering

I. INTRODUCTION

Convolutional neural network (CNN) has been widely used in recent years due to its remarkable performance in object detection and speech recognition. It was shown in [1]–[3] that deep convolutional neural network (DCNN) achieves remarkable accuracy in image classification. Recently, lots of research efforts [4], [5] have been devoted to improve the performance of DCNNs and reduce the gradient vanishing [6], [7] in the training process. Due to the fantastic performance of CNN, many computer vision applications also employ CNN to improve their performance. For example, CNN has achieved great performance in image annotation [8], visual QA system [9], 3D interpreter [10] and many other areas. Moreover, CNN was applied in speech recognition in [11] and was shown to achieve higher accuracy compared to previous methods.

DCNN performs well at the cost of dramatically increased computational complexity. Hence, efficient hardware implementation of these networks for real time processing is very challenging. The deep structure of DCNNs not only increases the computational complexity, but also incurs significant storage requirement. The weights and activations dominate the overall storage. Activations are the pixels of feature maps in a CNN. For the VGG-16 [2] net, the memory required to store all weights and activations is around 2Gb and 200Mb, respectively, when each weight and activation are half-precision floating-point numbers. In [12], the number of trained parameters of DCNNs has been reduced to less than 5% of their original size.

One important approach to reduce the storage requirement is to replace the full or half-precision floating-point number with fixed-point number for the computations of DCNNs. Researchers have proposed various fixed-point quantization schemes for the activations of DCNNs. A cross layer nonuniform quantization (CLNQ) scheme was proposed in [13] to minimize the number of bits required to store all activations. In [14], a nonuniform quantization scheme and the approximate computing technique were combined together to reduce the power consumption of a CNN. However, the number of required memory bits to store all activations is still very large even with these fixed-point quantization schemes.

In this paper, we focus on the efficient quantization of activations in a DCNN. The main contributions of this work are as follows.

- Two intra-layer nonuniform quantization (ILNQ) schemes, equal distance intra-layer nonuniform quantization (ENQ) scheme and K-means clustering based intra-layer nonuniform quantization (KNQ), are proposed for the quantization of activations in DCNNs. Compared to the state-of-the-art quantization scheme in [13], the proposed ILNQ schemes reduce the number of required memory bits to store all activations while maintaining almost the same accuracy.
- Compared to the ENQ scheme, the KNQ scheme improves the accuracy and slightly reduces the number of required memory bits at the cost of small hardware overhead when hardware implementations are considered. The KNQ scheme provides a tradeoff between hardware complexity and accuracy.
- Both the ENQ and KNQ schemes are applied to the quantization of VGG-16 and AlexNet [1] with the ILSVRC-2012 [15] data set. Compared to the quantization scheme in [13], it is demonstrated that both of the ENQ and KNQ schemes reduce the number of required memory bits to store all activations by approximately 50% while achieving almost the same or even better accuracy. Compared to the floating-point implementation, the accuracy loss is less than 2% for both of the ENQ and KNQ schemes.

The rest of the paper is organized as follows. Related works are discussed in Section II. The proposed intra-layer nonuniform quantization schemes are presented in Section III. The comparisons of different quantization methods and related discussions are provided in Section IV-C. At last, the conclu-

sions are drawn in Section V.

II. RELATED WORK

The quantization of DCNNs has been widely discussed in the open literatures. These works can be categorized into weight compression and activation quantization. Many previous works focus on weight compression of convolutional and fully-connect layers. A partial pruning algorithm was proposed in [16] to reduce the memory required by all weights. A compression method, which consists of pruning, quantization and Huffman coding, was proposed in [12] to compress the weights of a DCNN. The coding technology [17] was also employed to perform the quantization of DCNN as well. In [18], it was showed that the weight of fully-connected layers can be compressed by truncated singular value decomposition. A hash trick was proposed in [19] to compress the DCNN. Moreover, binary weights were employed in [20], [21] to reduce both computational complexity and storage requirement at the cost of certain accuracy loss. On the other hand, the quantization of activations has rarely been discussed. In [13], the signal-to-quantization noise ratio (SQNR) metric was employed to compute the number of quantization bits for each activation. The quantization of activations in the fully-connect layer was discussed in [22].

III. PROPOSED INTRA-LAYER NONUNIFORM QUANTIZATION OF DCNNs

The proposed ILNQ of DCNN is based on the empirical distributions of activations of each convolutional layer. The distribution of activation data for each layer of a CNN on the CIFAR-10 benchmark was shown in [13]. According to their experiments, the distribution of both activations and weights in most layers are roughly Gaussian distribution. To find out whether the distribution of activations in a deeper CNN is Gaussian-like distribution as well, we check the data of some deeper networks such as VGG-16 and AlexNet on the data set of ILSVRC-2012. Take the VGG-16 as an example, the distribution of activations with each layer is shown in Fig. 1, where the horizontal and vertical coordinates denote the magnitude and the corresponding probability, respectively. Note that the activations after ReLU are quantized in this paper. Since the ReLU function has non-negative output, all activations discussed in this paper are non-negative. As shown in Fig. 1, for VGG-16, the distribution of activations in each convolutional layer is Gaussian-like. Besides, most of the activations are zero for each convolutional layer shown in Fig. 1. Similar observations are obtained for the AlexNet based on the same data set.

A. Proposed ENQ and KNQ Schemes

The quantization process can be viewed as a mapping of activations to a set of quantization points (QPs), where each QP corresponds to a fixed-point value that will be used in the future computations. Let $\{P_0, P_1, \dots, P_{N-1}\}$ denote a set of QPs with N elements. For $i = 0, 1, \dots, N-1$, let V_i denote

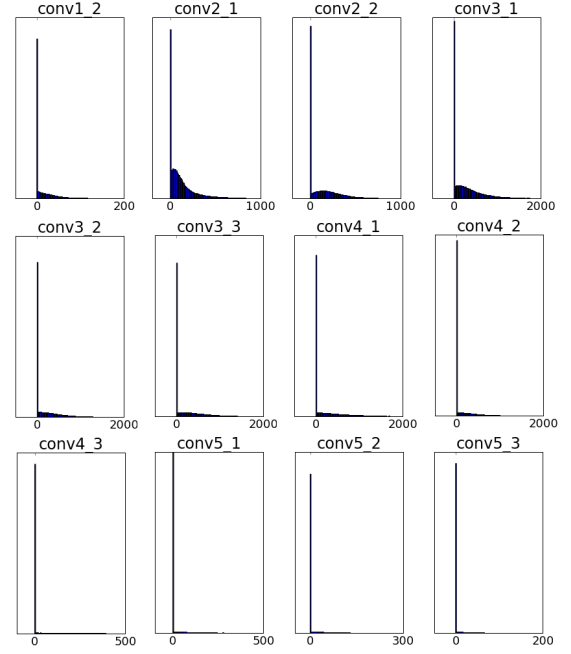


Fig. 1. Distribution of activations in VGG-16.

the corresponding fixed-point value associated with P_i . The quantization of an activation a is the following mapping:

$$a \rightarrow P_k, \quad (1)$$

where $k \in \{0, 1, \dots, N-1\}$. The storage of an quantized activation requires $K = \lceil \log_2 N \rceil$ bits. Let K' denote the number of bits used to store a V_i for $i = 0, 1, \dots, N-1$. It is possible that $K \neq K'$.

As shown in Fig. 1, it can be concluded that most activations within a layer are relatively small. It is reasonable to assign more QPs to represent the smaller activations without incurring obvious degradation of accuracy. In more detail, the proposed two ILNQ schemes are described as follows.

- For uniform quantization, i.e., each activation in a DCNN is quantized with q bits (2^q QPs in total). Note that all activations are non-negative since we are storing activations after the ReLU step. Let F denote the number of fractional bits in the q -bit uniform quantization. For the uniform quantization mentioned below in this paper, $V_i = i2^{-F}$ for $i = 0, 1, \dots, 2^q - 1$. For a DCNN, let A and A' denote the accuracy with floating and q -bit uniform quantization, respectively. The minimal value of q (denoted as q') is calculated such that $A - A' \leq \delta$, where δ is a small positive number determined by the corresponding data set and application.
- For activations within each layer i , the proposed ENQ scheme employs an E_i -bit nonuniform quantization scheme, where $E_i \leq q_m$. For the proposed E_i -bit ENQ scheme, there are 2^{E_i} QPs, $P_{i,0}, P_{i,1}, \dots, P_{i,2^{E_i}-1}$, where $P_{i,k}$ corresponds to the fixed-point value $V_{i,k} = k2^{q_m-E_i}2^{-F}$. Here, $k = 0, 1, \dots, 2^{E_i} - 1$. Supposing

the magnitude of an activation is x , the ENQ scheme quantizes it to $\lfloor \frac{x}{2^{q_m - E_i}} \rfloor$ if $x \leq 2^{q_m} - 1$. Otherwise, x is quantized to $2^{E_i} - 1$. Note that each activation within layer i is stored using E_i bits. When an activation is needed to participate in the convolutional computations in the next layer, it should be converted to a q_m -bit activation first based on the relationship between QPs and fixed-point values. In this paper, exhaustive search is employed to find the minimal E_i for each layer i such that the resulting accuracy is close to A' .

- Considering that the distribution of activations within a convolutional layer is Gaussian-like, the proposed ENQ scheme does not take full advantage of the distribution. The proposed KNQ scheme employs K-means clustering method to assign each QP with a fixed-point value. Let S denote the set of all activations within convolutional layer i . Suppose T_i bits are used to quantize all these activations. Let $S_0, S_1, \dots, S_{2^{T_i}-1}$ be 2^{T_i} non-overlap sets which divide the whole set S , where $\cup_{k=0}^{2^{T_i}-1} S_k = S$. For a given T_i , the proposed KNQ scheme first finds 2^{T_i} fixed-point values, $d_0, d_1, \dots, d_{2^{T_i}-1}$, by solving the following problem with the K-means clustering method:

$$\min_{d_0, d_1, \dots, d_{2^{T_i}-1}} \sum_{k=0}^{2^{T_i}-1} \sum_{j=0}^{|S_k|-1} |s_{k,j} - d_k|^2, \quad (2)$$

where $|S_j|$ denotes the number of elements in S_j and $s_{k,j} \in S_k$. Once these 2^{T_i} values are determined, x is quantized to k if $d_k \leq x < d_{k+1}$. If $x \geq d_{2^{T_i}-1}$, x is quantized to $2^{T_i} - 1$. For $k = 0, 1, \dots, 2^{T_i} - 1$, quantization point $P_{i,k}$ corresponds to d_k . Similar to the ENQ method, a quantized activation will be mapped to the corresponding fixed-point value first when it is needed in the future computation.

For the KNQ scheme, in order to reduce the accuracy loss, the set S is pre-processed in this paper. All activations larger than a threshold value M is saturated to M . In this paper, $M = (2^{q_m} - 1)2^{-F}$, since the uniform quantization demonstrates that considering larger q_m is not necessary.

B. Proposed Data Conversion Units

In terms of hardware implementation, compared to the uniform quantization scheme and the quantization scheme in [13], the proposed ENQ and KNQ schemes need extra circuits to convert between QPs and corresponding fixed-point values. In this paper, the efficient data conversion hardware architectures for the ENQ and KNQ schemes are proposed in Figs. 2 and 3, respectively. Let w_1 and w_2 denote a fixed-point value and the corresponding quantization point. For the ENQ scheme, the quantization unit of ENQ (QE) is in Fig. 2(a), where C is the number of different quantization bits and $L_i dx$ is the index of the convolutional layer. The DEC1 unit takes $L_i dx$ as input to generate selection signal for the multiplexor. The right shift (RS) unit shift the input to right by a bits. The conversion unit for ENQ (CE) is shown in Fig. 2(b), where the left shift (LS) unit shifts the input to left by a bits.

Let M denote the number of centroid values generated by the K-means clustering method. The QC of KNQ (QK) is shown in Fig. 3(a), where cmp is a comparator. DEC₂ is a priority encoder unit which generates the quantized value. As shown in Fig. 3(b), the conversion unit for KNQ (CK) can be implemented with a multiplexor which selects out the corresponding centroid values for the input QP.

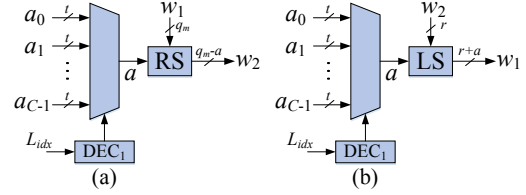


Fig. 2. QU and conversion unit for ENQ.

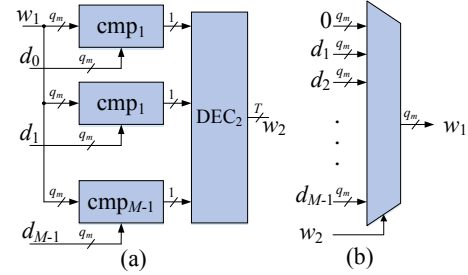


Fig. 3. QU and conversion unit for KNQ.

IV. NUMERICAL RESULTS AND COMPARISONS

In this paper, based on the ILSVRC-2012 data set, the proposed ILNQ schemes are applied on the VGG-16 and AlexNet. The VGG-16 achieves remarkable performance on image classification and its deep structure can be modified to adapt to various applications. Moreover, the size of activations in the VGG-16 is very huge. Hence, VGG-16 is a typical representation of DCNNs. For all the implementations in this paper, all the weights and bias take a 14-bit uniform quantization.

A. Uniform Quantization and Cross-Layer Nonuniform Quantization

We first perform the uniform quantization of VGG-16 according to the distribution shown in Fig. 1. As shown in Table I, the accuracy of the full precision is 88.5%. We use the same bit-width for all layers without fine-tuning. According to our observations, some activations are even larger than 15000. However, 12 bits are enough for the uniform quantization of all activations.

TABLE I
UNIFORM QUANTIZATION OF VGG-16

Quantization bit	14	13	12	11	10	9
Top5 Accuracy(%)	88.4	88.4	88.5	87.0	79.6	56.0

TABLE II
ENQ OF VGG-16 PART 1

Top5 Accuracy(%)	Index	conv1_1	conv1_2	conv2_1	conv2_2	conv3_1	conv3_2	conv3_3	conv4_1	conv4_2	conv4_3
56.60	1	8	4	5	5	5	5	5	5	5	5
79.43	2	8	4	5	5	5	5	5	5	5	5
83.46	3	8	4	5	5	5	5	5	5	5	5
85.81	4	8	5	6	4	6	6	6	6	6	6
86.19	5	8	5	6	5	5	4	6	6	6	6
86.25	6	8	5	6	5	5	5	5	5	5	5

TABLE III
ENQ OF VGG-16 PART 2

Top5 Accuracy(%)	Index	conv5_1	conv5_2	conv5_3	fc6	fc7	fc8
56.60	1	5	4	4	3	2	2
79.43	2	5	4	4	4	2	2
83.46	3	5	4	4	6	3	2
85.81	4	6	5	5	6	3	2
83.46	5	6	5	5	6	3	2
86.25	6	6	5	5	6	3	2

TABLE IV
K-MEANS

	d_0	d_1	d_2	d_3	d_4	d_5	d_6	d_7	d_8	d_9	d_{10}	d_{11}	d_{12}	d_{13}	d_{14}	d_{15}
conv1_2	0	0	0	0	0	0	0	0	0	0	0	0	0	1	3	6
conv2_1	0	11	22	35	49	64	80	97	115	134	154	176	200	226	254	284
conv2_2	0	23	46	69	92	115	138	161	185	210	236	263	292	323	356	391
conv3_1	0	45	91	138	186	235	285	338	394	453	516	583	653	726	803	886
conv3_2	0	45	90	136	183	232	282	333	386	441	498	558	621	689	763	843
conv3_3	0	48	97	146	196	247	299	352	407	464	523	585	649	716	786	860
conv4_1	0	55	113	172	233	297	361	426	494	566	641	720	801	886	973	1066
conv4_2	0	44	88	133	179	227	277	329	385	443	504	567	632	703	779	862
conv4_3	0	35	71	109	149	191	235	282	333	388	447	513	586	667	760	867
conv5_1	0	28	58	91	129	169	215	267	323	384	452	527	612	713	824	952
conv5_2	0	16	34	54	77	103	132	165	203	247	296	356	425	499	585	687
conv5_3	0	10	22	36	52	71	93	119	148	177	211	248	288	330	370	415
	d_{16}	d_{17}	d_{18}	d_{19}	d_{20}	d_{21}	d_{22}	d_{23}	d_{24}	d_{25}	d_{26}	d_{27}	d_{28}	d_{29}	d_{30}	d_{31}
conv1_2	10	15	21	28	36	45	56	69	85	105	128	156	191	234	290	373
conv2_1	316	350	387	426	468	514	563	616	674	739	814	901	1015	1162	1407	1815
conv2_2	429	470	517	569	628	695	772	863	970	1094	1245	1432	1666	1977	2425	3082
conv3_1	977	1075	1181	1299	1428	1570	1730	1908	2092	2286	2517	2760	3041	3394	3834	4096
conv3_2	930	1024	1128	1243	1368	1505	1655	1818	2000	2216	2466	2730	3013	3368	3821	4096
conv3_3	940	1027	1120	1222	1334	1457	1598	1757	1941	2151	2391	2662	2983	3357	3820	4096
conv4_1	1164	1270	1384	1505	1635	1775	1927	2094	2266	2473	2703	2943	3215	3525	3893	4096
conv4_2	956	1062	1178	1302	1437	1584	1752	1946	2152	2397	2653	2959	3250	3551	3888	4096
conv4_3	988	1128	1285	1465	1680	1945	2229	2527	2914	3130	3282	3419	3563	3754	4004	4096
conv5_1	1095	1265	1457	1669	1840	2004	2086	2143	2264	2371	2485	2570	2671	2813	2867	2998
conv5_2	790	926	1037	1160	1287	1349	1413	1509	1569	1634	1700	1772	1830	1896	1998	2074
conv5_3	457	513	553	594	632	662	693	732	757	793	812	849	893	914	943	987

For the cross-layer nonuniform quantization, the exhaustive search is employed. Since there are 13 convolutional layers in the VGG-16, the combination of quantization bits, which achieves the best tradeoff between accuracy and the size of all activations, is (8, 8, 10, 11, 11, 11, 11, 11, 10, 10, 9, 8). The quantization results on the AlexNet is similar to that in [13].

B. ENQ and KNQ Schemes

For the VGG-16, the numbers of quantization bits generated by the ENQ scheme are shown in Tables II and III, where several combinations of E_i 's and the corresponding accuracy are shown. Index 6 is the combination which achieves the best

tradeoff between accuracy and the number of required memory bits.

The results generated by the KNQ scheme on VGG-16 and AlexNet are shown in Tables IV and VI. As shown in Table IV, $E_i = 5$ for each convolutional layer i in the VGG-16. The corresponding computed 32 centroid fixed-point numbers for each convolutional layer are shown in Table IV. For the AlexNet, $E_i = 3$ for each convolutional layer i . The centroid fixed-point numbers are not shown here for simplicity. Besides, for both VGG-16 and AlexNet, the pre-processing can improve the accuracy as shown in Table VI.

In this paper, the proposed quantization unit and data conversion unit for VGG-16 are implemented based a TSMC

90nm CMOS technology.

TABLE V
AREA AND CRITICAL PATH DELAY

	QE	CE	QK	CK
area (μm^2)	776	311	7512	4087
CPD (ns)	0.43	0.25	0.65	0.31

C. Comparisons and Discussions

In Table VII, we compare the proposed ENQ and KNQ schemes with the cross-layer nonuniform quantization scheme [13] in terms of accuracy and the number of required bits to store all activations. As shown in Table VII, NB denotes the number of bits required to store all activations and NNB denotes the normalized NB. As shown in Table VII, compared to that in [13], both of our quantization schemes reduce the number of required memory bits by around 50% for both considered DCNNs. On the other hand, for the VGG-16, the ENQ and KNQ schemes increase the accuracy by 0.03% and 0.36% compared to the scheme in [13], respectively. For the AlexNet, the accuracy of ENQ and KNQ schemes is slightly worse than that of the scheme in [13].

TABLE VI
K-MEANS CLUSTERING QUANTIZATION

	no pre-process		with pre-process	
Bit-width for VGG-16	4	5	4	5
Top5 Accuracy of VGG-16(%)	62.8	85.8	69.57	86.58
Bit-width for AlexNet	2	3	2	3
Top5 Accuracy of AlexNet(%)	34.41	77.55	39.03	78.23

TABLE VII
COMPARISON WITH [13]

VGG-16 Net				
	Half-precision	ENQ	KNQ	[13]
Accuracy(%)	88.4	86.25	86.58	86.22
NB (MB)	27	9.5	8.4	16.8
NNB	1.6	0.56	0.50	1
Alex Net				
	Half-precision	ENQ	KNQ	[13]
Accuracy(%)	79.95	77.55	78.23	78.87
NB (MB)	2.57	0.48	0.48	1.12
NNB	2.29	0.43	0.43	1

As shown in Fig. 1, most of activations are 0 after ReLU computing. With various data compression techniques, the number of required memory bits can be reduced in further. Besides, it is believed that the fine-tuning can help improve the accuracy.

V. CONCLUSION

In this paper, we have applied several methods on the quantization of DCNN including the VGG-16 and AlexNet. It has been demonstrated that only 5 and 3 bits are needed for quantizing activations of the VGG-16 and AlexNet, respectively. Compared to the state-of-the-art quantization schemes,

the proposed ENQ and KNQ schemes achieve significant reductions on the required memory storage for activations. The memory saving feature of the proposed schemes will facilitate the embedded hardware implementations of DCNNs.

REFERENCES

- [1] A. Krizhevsky, I. Sutskever, and G. E. Hinton, "Imagenet classification with deep convolutional neural networks," in *Advances in neural information processing systems*, 2012, pp. 1097–1105.
- [2] K. Simonyan and A. Zisserman, "Very deep convolutional networks for large-scale image recognition," *arXiv preprint arXiv:1409.1556*, 2014.
- [3] K. He, X. Zhang, S. Ren, and J. Sun, "Deep residual learning for image recognition," *arXiv preprint arXiv:1512.03385*, 2015.
- [4] N. Srivastava, H. Georey, A. Krizhevsky, I. Sutskever, and R. Salakhutdinov, "Dropout: A simple way to prevent neural networks from overfitting," *Journal of Machine Learning Research*, vol. 15, pp. 1929–1958, 2014.
- [5] S. Ioffe and C. Szegedy, "Batch normalization: Accelerating deep network training by reducing internal covariate shift," 2015.
- [6] D. Erhan, P. Manzagol, Y. Bengio, S. Bengio, and P. Vincent, "The difficulty of training deep architectures and the effect of unsupervised pre-training," 2009.
- [7] X. Glorot and Y. Bengio, "Understanding the difficulty of training deep feedforward neural networks," *Journal of Machine Learning Research*, 2010.
- [8] A. Karpathy and L. Fei-Fei, "Deep visual-semantic alignments for generating image descriptions," in *Proceedings of the IEEE Conference on Computer Vision and Pattern Recognition*, 2015, pp. 3128–3137.
- [9] S. Antol, A. Agrawal, J. Lu, M. Mitchell, D. Batra, Z. C. Lawrence, and D. Parikh, "Vqa: Visual question answering," in *Proceedings of the IEEE International Conference on Computer Vision*, 2015, pp. 2425–2433.
- [10] J. Wu, T. Xue, J. J. Lim, Y. Tian, J. B. Tenenbaum, A. Torralba, and W. T. Freeman, "Single image 3d interpreter network," *arXiv preprint arXiv:1604.08685*, 2016.
- [11] D. Amodei, R. Anubhai, E. Battenberg, C. Case, J. Casper, B. Catanzaro, J. Chen, M. Chrzanowski, A. Coates, G. Diamos, et al., "Deep speech 2: End-to-end speech recognition in english and mandarin," *arXiv preprint arXiv:1512.02595*, 2015.
- [12] S. Han, H. Mao, and W. J. Dally, "Deep compression: Compressing deep neural network with pruning, trained quantization and Huffman coding," *CoRR, abs/1510.00149*, vol. 2, 2015.
- [13] D. D. Lin, S. S. Talathi, and V. S. Annapureddy, "Fixed point quantization of deep convolutional networks," *arXiv preprint arXiv:1511.06393*, 2015.
- [14] B. Moons, B. De Brabandere, L. Van Gool, and M. Verhelst, "Energy-efficient convnets through approximate computing," in *2016 IEEE Winter Conference on Applications of Computer Vision (WACV)*. IEEE, 2016, pp. 1–8.
- [15] O. Russakovsky, J. Deng, H. Su, J. Krause, S. Satheesh, S. Ma, Z. Huang, A. Karpathy, A. Khosla, M. Bernstein, A. C. Berg, and F.-F. Li, "ImageNet Large Scale Visual Recognition Challenge," *International Journal of Computer Vision (IJCV)*, vol. 115, no. 3, pp. 211–252, 2015.
- [16] S. Anwar, K. Hwang, and W. Sung, "Structured pruning of deep convolutional neural networks," *arXiv preprint arXiv:1512.08571*, 2015.
- [17] Y. Gong, L. Liu, M. Yang, and L. Bourdev, "Compressing deep convolutional networks using vector quantization," 2014.
- [18] E. Denton, W. Zaremba, J. Bruna, Y. Lecun, and R. Fergus, "Exploiting linear structure within convolutional networks for efficient evaluation," 2014.
- [19] W. Chen, J. T. Wilson, S. Tyree, K. Q. Weinberger, and Y. Chen, "Compressing neural networks with the hashing trick," 2015.
- [20] M. Courbariaux, Y. Bengio, and J. David, "Binaryconnect: Training deep neural networks with binary weights during propagations," 2015.
- [21] M. Rastegari, V. Ordonez, J. Redmon, and A. Farhadi, "Xnor-net: Imagenet classification using binary convolutional neural networks," 2016.
- [22] K. Hwang and W. Sung, "Fixed-point feedforward deep neural network design using weights +1, 0, and 1," 2014.